Electron doping evolution of structural and antiferromagnetic phase transitions in $NaFe_{1-x}Co_xAs$ iron pnictides

Guotai Tan,[1] Yu Song,[2] Chenglin Zhang,[2] Lifang Lin,[1] Zhuang Xu,[1] Tingting Hou,[1] Wei Tian,[3] Huibo Cao,[3] Shiliang Li,[4,5] Shiping Feng,[1] and Pengcheng Dai[2,1,*]

[1]*Department of Physics, Beijing Normal University, Beijing 100875, China*

[2]*Department of Physics and Astronomy, Rice University, Houston, Texas 77005, USA*

[3]*Quantum Condensed Matter Division, Oak Ridge National Laboratory, Oak Ridge, Tennessee 37831, USA*

[4]*Beijing National Laboratory for Condensed Matter Physics, Institute of Physics, Chinese Academy of Sciences, Beijing 100190, China*

[5]*Collaborative Innovation Center of Quantum Matter, Beijing, China*

(Received 10 April 2016; revised manuscript received 3 June 2016; published 13 July 2016)

We use transport and neutron diffraction to study the electronic phase diagram of $NaFe_{1-x}Co_xAs$. In the undoped state, NaFeAs exhibits a tetragonal-to-orthorhombic structural transition below T_s followed by a collinear antiferromagnetic (AF) order below T_N. Upon codoping to form $NaFe_{1-x}Co_xAs$, T_s and T_N are gradually suppressed, leading to optimal superconductivity near Co-doping $x = 0.025$. While transport experiments on these materials reveal an anomalous behavior suggesting the presence of a quantum critical point (QCP) near optimal superconductivity, our neutron diffraction results indicate that commensurate AF order becomes transversely incommensurate with $T_N > T_c$ before vanishing abruptly at optimal superconductivity. These results are remarkably similar to electron-doping and isovalent-doping evolution of the AF order in $BaFe_{2-x}Ni_xAs_2$ and $BaFe_2(As_{1-x}P_x)_2$, thus suggesting a universal behavior in the suppression of the magnetic order in iron pnictides as superconductivity is induced.

DOI: 10.1103/PhysRevB.94.014509

I. INTRODUCTION

High-transition-temperature (high-T_c) superconductivity in copper oxides [1] and iron pnictides [2–5] generally appears in the vicinity of a magnetically ordered phase. For this reason, magnetism is believed to play a critical role in the pairing mechanisms of high-T_c superconductors [4]. In the case of copper oxides, hole doping to La_2CuO_4 by partially substituting La by Sr will gradually suppress the static antiferromagnetic (AF) order before superconductivity emerges [6]. For iron pnictide superconductors such as electron-doped $BaFe_{2-x}T_xAs_2$ (T = Co, Ni) [7–13] and isovalent-doped $BaFe_2(As_{1-x}P_x)_2$ [14–18], optimal superconductivity appears near the regime where the static collinear AF order [Fig. 1(a)] is suppressed. While transport measurements have suggested the presence of a quantum critical point (QCP) in $BaFe_{2-x}T_xAs_2$ [12,19] and $BaFe_2(As_{1-x}P_x)_2$ [20], as revealed by the linear temperature dependence of the resistivity near optimal superconductivity, neutron scattering experiments instead find that the static AF order in $BaFe_{2-x}Ni_xAs_2$ and $BaFe_2(As_{1-x}P_x)_2$ families of materials always has T_N above T_c and disappears in a weakly first-order fashion abruptly near optimal superconductivity, suggesting an avoided QCP [12,13,17,18]. On the other hand, recent neutron scattering [21,22] and Mössbauer spectroscopy [23] experiments on hole-doped iron pnictides $(Ba,Sr)_{1-x}Na_xFe_2As_2$ family of materials found a new magnetically ordered state with restored tetragonal symmetry near optimal superconductivity, replacing the stripe AF ordered state of the undoped $BaFe_2As_2$ [24]. These results suggest that the static AF order in iron pnictides display a plethora of interesting behaviors near optimal superconductivity. In order to understand the relationship between magnetism and superconductivity, it is important to systematically study the electronic phase diagrams of different classes of iron pnictides and establish their universal features.

In this article, we report systematic neutron diffraction experiments on Co-doped $NaFe_{1-x}Co_xAs$ iron pnictides. Although previous transport, μSR, and heat capacity experiments have established the phase diagram of $NaFe_{1-x}Co_xAs$ [25–30], there are no systematic neutron diffraction measurements on $NaFe_{1-x}Co_xAs$ to determine the Co-doping evolution of the AF order and compare with those of electron, hole, and isovalently doped $BaFe_2As_2$ [12,13,17,18]. Figure 1(c) summarizes the phase diagram of $NaFe_{1-x}Co_xAs$ determined from our transport and neutron diffraction experiments on single-crystal samples. In addition to the well known gradual suppression of structural and AF order with increasing Co doping ($T_s > T_N > T_c$), our data reveal a commensurate-to-incommensurate transition in static AF order before it vanishes abruptly near optimal superconductivity. Although transport measurements on $NaFe_{1-x}Co_xAs$ show linear temperature dependence of the resistivity near optimal superconductivity suggestive of a QCP, the first-order-like disappearing nature of the AF order with increasing Co doping indicates an avoided QCP. These results are remarkably similar to electron-doped $BaFe_{2-x}T_xAs_2$ [7–10,12,13], thus suggesting a universal electronic phase diagram for electron-doped $BaFe_2As_2$ and NaFeAs iron pnictides in spite of their differences in crystal and electronic structures.

II. EXPERIMENTAL RESULTS

High-quality $NaFe_{1-x}Co_xAs$ single crystals with nominal doping level x were synthesized by the self-flux method as described elsewhere [30]. Similar to previous work [32], we use inductively coupled plasma (ICP) atomic-emission spectroscopy measurements to determine the chemical

*pdai@rice.edu

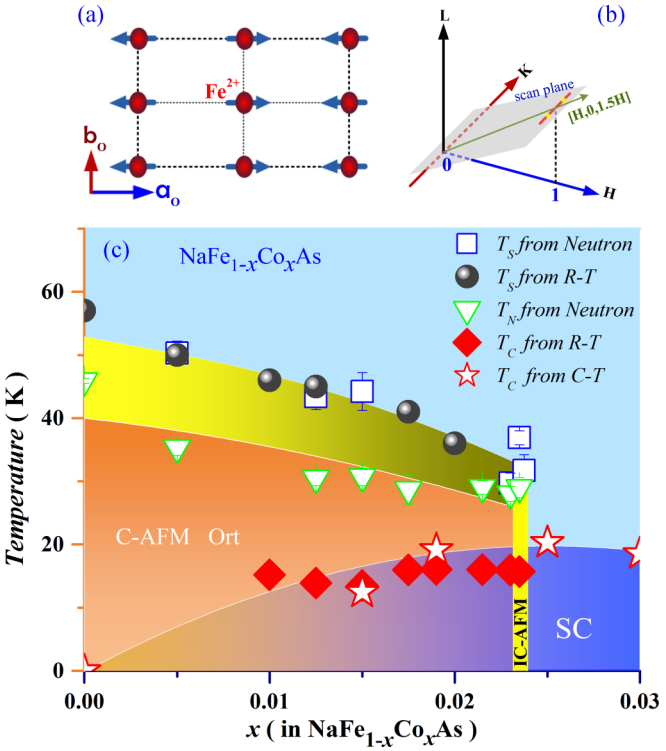

FIG. 1. The magnetic structure, neutron scattering geometry, and phase diagram of $NaFe_{1-x}Co_xAs$ as determined from transport and neutron diffraction experiments. (a) The in-plane magnetic structure of NaFeAs [31]. a_o and b_o ($a_o > b_o$) are orthorhombic crystal axes in the AF ordered state. (b) Neutron scattering geometry used to search for transverse incommensurate AF order for samples near optimal superconductivity. The scattering plane is $[0,K,0] \times [H,0,1.5H]$, and the scan direction to search for incommensurate magnetic order is along the $[1,K,1.5]$ direction shown the dashed line. (c) The phase diagram of $NaFe_{1-x}Co_xAs$, where Ort, Tet, and SC indicate the orthorhombic, tetragonal, and superconducting phases, respectively. The C-AFM and IC-AF denote commensurate and incommensurate AF order, respectively. The green down-pointing triangles and blue squares are T_N and T_s, respectively, determined from neutron diffraction experiments. The diamonds and stars are T_c determined from resistivity (R-T) and heat capacity (C-T), respectively [30].

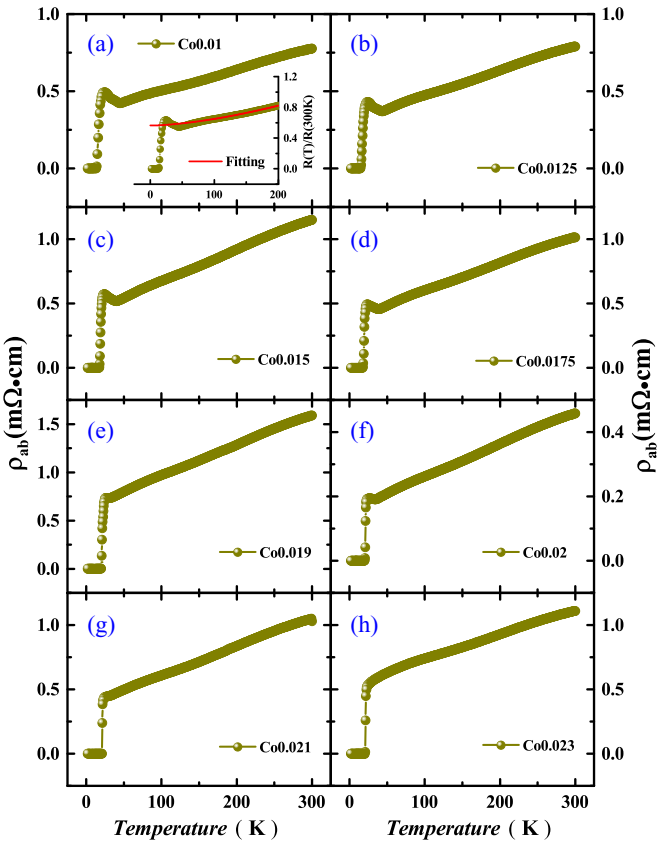

FIG. 2. Temperature dependence of the resistivity as a function of increasing Co doping for $NaFe_{1-x}Co_xAs$ with (a) $x = 0.01$, (b) 0.012 5, (c) 0.015, (d) 0.017 5, (e) 0.019, (f) 0.02, (g) 0.021, and (h) 0.023. The red solid line in the inset is a fit to the model: $\rho(T) = \rho_0 + AT^n$ up to 220 K in the normal state.

compositions of the samples. For the nominal $NaFe_{0.975}Co_{0.025}As$ samples, which contain an unknown amount of NaAs flux, ICP measurements suggest a total chemical composition of $Na_{0.94}Fe_{0.89}Co_{0.02}As$. Since the Na concentration of 0.94 is similar to the combined Fe and Co concentration of 0.91, we assume that the actual chemical compositions of $NaFe_{1-x}Co_xAs$ are similar to the nominal doping levels and quote the nominal doping level throughout the paper [32]. Resistivity measurements were carried out with the four-probe method using a physical property measurement system (PPMS). Neutron diffraction experiments were carried out on HB-1A thermal triple-axis spectrometer at the High-Flux Isotope reactor (HFIR), Oak Ridge National Laboratory. We define the wave vector **Q** at (q_x,q_y,q_z) as $(H,K,L) = (q_x a_o/2\pi, q_y b_o/2\pi, q_z c/2\pi)$ in reciprocal lattice units (rlu), where $a_o \approx b_o \approx 5.56$ Å, and $c = 6.95$ Å. In this orthorhombic unit cell notation, the collinear AF order in NaFeAs and Co-doped samples should occur at $\mathbf{Q}_{AF} = (1,0,L)$ where $L = 0.5, 1.5, \ldots$ rlu [31].

Figure 2 summarizes temperature dependence of the in-plane resistivity measurements for $NaFe_{1-x}Co_xAs$ with $x = 0.01, 0.0125, 0.015, 0.0175, 0.019, 0.02, 0.021$, and 0.023. The resistivity is normalized to the room temperature value per $\rho_{ab}(T)/\rho_{ab}(300\text{ K})$ in the inset of Fig. 2(a). For all measured Co-doping levels, $\rho_{ab}(T)/\rho_{ab}(300\text{ K})$ is metallic in the paramagnetic state, and the upturns above T_c for lightly Co-doped samples are due to structural and magnetic phase transitions [12,19]. To compare the resistivity behavior in $NaFe_{1-x}Co_xAs$ with those of the doped $BaFe_2As_2$ family of materials [12,19,33], we performed fits for the data from $T_s + 10$ K to 220 K using the empirical model [12,19,33,34]: $\rho(T) = \rho_0 + AT^n$, where ρ_0 is a constant, A is amplitude, and n is the temperature exponent. For a typical Fermi liquid metal, one expects $n = 2$, and a material close to QCP typically has $n = 1$ with $n < 2$, suggesting non-Fermi liquid behavior [35,36]. The red solid line in the inset of Fig. 2(a) represents a fit to the resistivity data. The Co-doping dependence of the fitting exponent n is shown in Fig. 3(e), which has a minimum value of $n \approx 1.3$ around $x \approx 0.02$ near optimal superconductivity. These results are similar to previous transport measurements on $NaFe_{1-x}Co_xAs$ [28,29] and

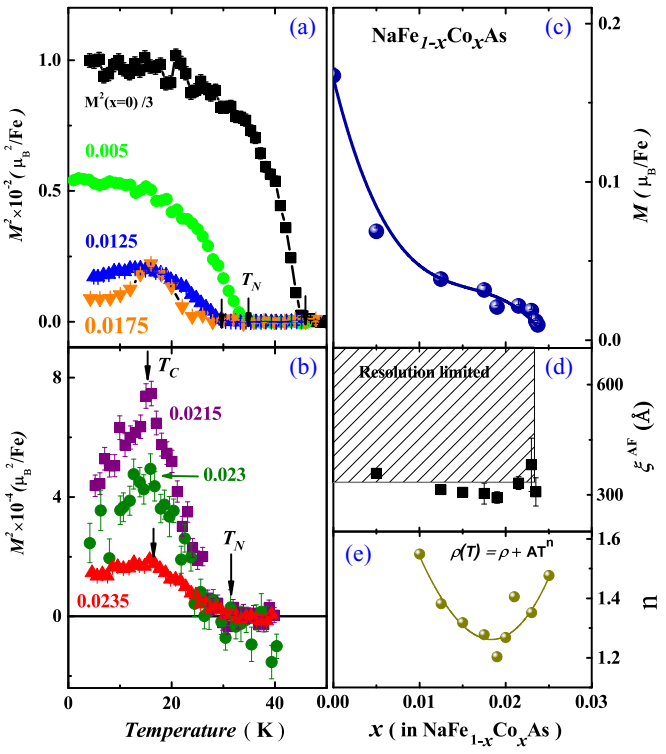

FIG. 3. Temperature dependence of the magnetic order parameters normalized to a weak nuclear Bragg peak (2,0,0) for $NaFe_{1-x}Co_xAs$ with (a) $x = 0,0.005,0.012\,5,0.017\,5$, and (b) $0.021\,5$, 0.023, and $0.023\,5$. The negative values are due to imperfect high-temperature background scattering subtraction. (c) The Co-doping dependence of the ordered magnetic moment. (d) The spin-spin correlation length in Å as a function of Co doping. The shaded area indicates that spin-spin correlation length is resolution limited. (e) Co-doping dependence of the exponent n from fits to the resistivity data.

suggest the presence of a QCP near optimal superconductivity in $NaFe_{1-x}Co_xAs$ similar to that of $BaFe_{2-x}T_xAs_2$.

Figures 3(a) and 3(b) summarize the magnetic order parameters for $NaFe_{1-x}Co_xAs$ with $x = 0.0,0.005$, $0.012\,5,0.017\,5,0.021\,5,0.021,0.023$, and $0.023\,5$. The magnetic scattering has been normalized to a weak nuclear Bragg peak (2,0,0) in the orthorhombic notation, thus giving the ordered moment square M^2 in units of μ_B^2/Fe. In previous neutron diffraction work on $Na_{1-\delta}FeAs$ [25,31], the Fe ordered moment is estimated to be $M = 0.09 \pm 0.04\ \mu_B$/Fe, which is somewhat smaller than $M = 0.17 \pm 0.034\ \mu_B$/Fe in the present NaFeAs. This is most likely due to the fact that previous work was carried out on slightly Na deficient samples, and the air sensitivity nature of the $NaFe_{1-x}Co_xAs$ samples was not fully recognized [37]. Figure 3(a) shows the data for $x = 0.0,0.005,0.012\,5$, and $0.017\,5$. With increasing Co doping, we can see a clear reduction in magnetic ordered moment and T_N. For Co-underdoped bulk superconducting samples, including $x = 0.017\,5,0.021\,5,0.023$, and $0.023\,5$, there is also a reduction of the AF ordered moment below T_c, indicating a competing static AF order with superconductivity similar to underdoped $BaFe_{2-x}T_xAs_2$ [8,9]. In addition, the magnetic ordered moment decreases systematically with increasing Co doping, as illustrated in Fig. 3(c). The AF ordering temperature, however, seems to saturate around $T_N \approx 30$ K on approaching optimal superconductivity with $x = 0.023\,5$. We also note that the AF phase transitions become rounded for samples near optimal superconductivity. This is consistent with the temperature dependence of the magnetic order parameters of underdoped $BaFe_{2-x}T_xAs_2$ near optimal superconductivity, which has been attributed to a cluster spin glass state [38–40].

To determine Co-doping dependence of the spin-spin correlation length in the AF ordered phase of $NaFe_{1-x}Co_xAs$, we carried out neutron diffraction measurements in two different scattering geometries. For the underdoped sample where we expect the static AF order to be commensurate, we aligned the single crystals in the $[H,0,0] \times [0,0,L]$ scattering plane. For Co-doping level x near optimal superconductivity, we aligned the crystals in the $[0,K,0] \times [H,0,1.5H]$ scattering plane as shown in Fig. 1(b) in order to search for possible transverse incommensurate magnetic order, as seen in $BaFe_{2-x}T_xAs_2$ [11,12]. For lightly Co-doped $NaFe_{1-x}Co_xAs$, Fourier transforms of longitudinal scans along the $[H,H,0]$ direction reveal that spin-spin correlation lengths are resolution limited and greater than or equal to 290 Å [Fig. 3(d)]. This is the case for all samples probed.

Figures 4(a) and 4(b) show transverse and longitudinal scans, respectively, for $NaFe_{1-x}Co_xAs$ with $x = 0.012\,5$ at different temperatures. The scattering is featureless at $T = 45$ K (above T_N) along both directions. On cooling to $T = 15$ K and 5 K, we see clear magnetic scattering at commensurate

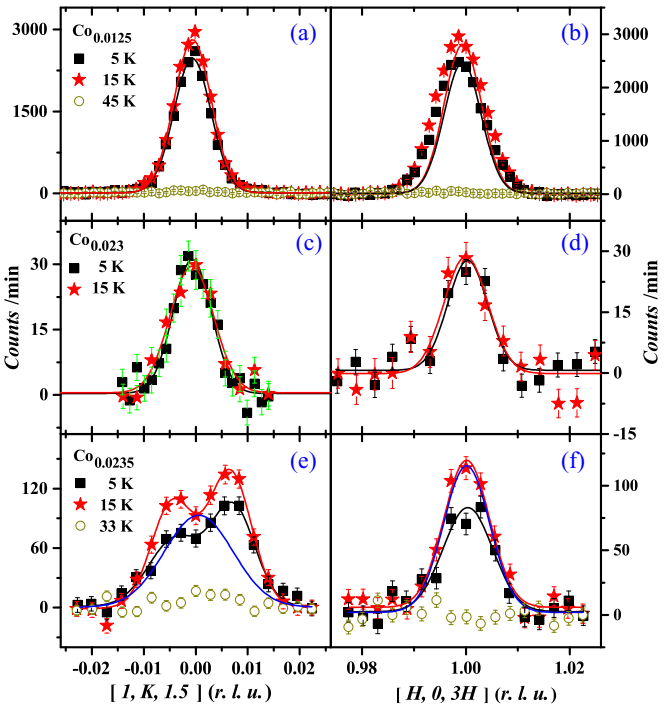

FIG. 4. Transverse and radial scans through the AF ordering wave vector $\mathbf{Q}_{AF} = (1,0,1.5)$ at different temperatures using scattering geometry as shown in Fig. 1(b). Transverse scans along the $[1,K,1.5]$ direction at different temperatures for $NaFe_{1-x}Co_xAs$ with (a) $x = 0.025$, (c) 0.023, and (e) $0.023\,5$. The corresponding longitudinal scans are shown in (b), (d), and (f), respectively. The blue solid line in (e) shows a fit to data obtained using $\lambda/2$ above T_N. The solid lines are Gaussian fits to the data on linear backgrounds.

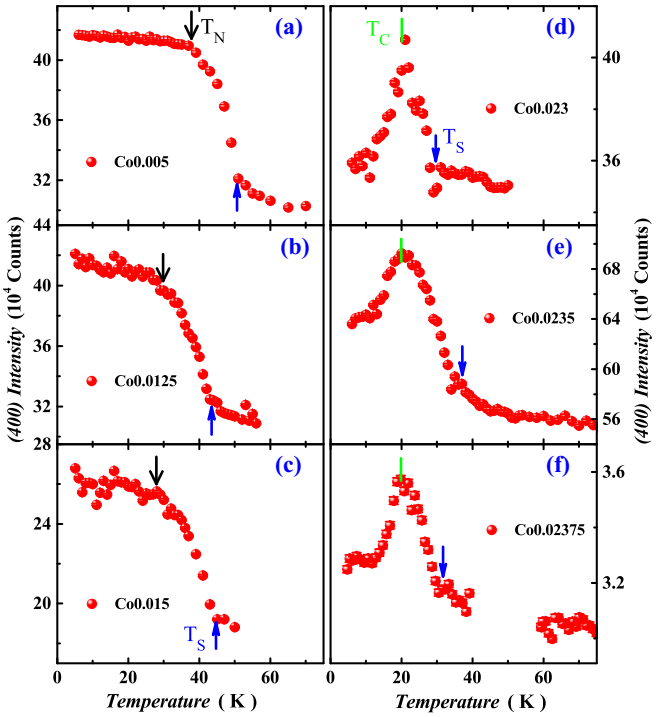

FIG. 5. Temperature dependence of a strong nuclear Bragg peak scattering (4,0,0) as a function of Co doping (a) $x = 0.005$, (b) 0.012 5, (c) 0.015, (d) 0.023, (e) 0.023 5, and (f) 0.023 75. The blue vertical arrows mark estimated T_s. The black arrows mark T_N determined from neutron diffraction measurement, and the green arrows are T_c determined from transport data.

positions along the longitudinal and transverse directions [Figs. 4(a) and 4(b)]. The situation is similar for the $x = 0.023$ sample [Figs. 4(c) and 4(d)]. However, the transverse scans for the $x = 0.023\,5$ sample show two incommensurate peaks at $T = 15$ K and 5 K [Fig. 4(e)], while longitudinal scans are commensurate at all measured temperatures [Fig. 4(f)]. The positions of incommensurate peaks are similar to those of electron-doped $BaFe_{2-x}T_xAs_2$ [11,12]. These results thus suggest that the presence of transverse incommensurate magnetic order before optimal superconductivity may be a common feature of electron-doped $BaFe_2As_2$ and NaFeAs.

To determine electron-doping evolution of the orthorhombic-to-tetragonal structural transition in $NaFe_{1-x}Co_xAs$, we measured the temperature dependence of the intensity at the (4,0,0) nuclear Bragg reflection position in the orthorhombic notation [7]. From previous neutron diffraction experiments on $BaFe_2As_2$, we know that the intensity of the (4,0,0) nuclear Bragg reflection [or the nuclear Bragg peak (2,2,0) in the tetragonal notation] shows a dramatic jump at T_s arising from the neutron extinction release that occurs due to strain and domain formation related to the orthorhombic distortion [41,42]. Figure 5 summarizes the key results for $NaFe_{1-x}Co_xAs$ with $x = 0.005, 0.012\,5, 0.015, 0.023, 0.023\,5$, and 0.023 75. In all cases, we see a clear enhancement of the scattering intensity below a characteristic temperature marked by vertical arrows. The resulting T_s as a function of Co doping is plotted together with other information shown in Fig. 1(c), thus establishing the Co-doping dependence of the $NaFe_{1-x}Co_xAs$ phase diagram.

III. CONCLUSION

To summarize, we have mapped out the orthorhombic-to-tetragonal structural and AF ordering phase transition phase diagram in $NaFe_{1-x}Co_xAs$ as a function of Co doping up to optimal superconductivity. In spite of the rather different electron and hole Fermi surfaces between electron-doped $BaFe_{2-x}T_xAs_2$ [43] and $NaFe_{1-x}Co_xAs$ [44–46], we show that the Co-doping evolutions of the structural and magnetic phase transitions in these two classes of materials are remarkably similar. These results confirm the universal nature of the Co-doping dependence of the structure and magnetic phase transitions and suggest that the AF order vanishes in the first-order fashion with an avoided magnetic QCP in iron pnictides. Since inelastic neutron scattering experiments on these two families of iron-based superconductors reveal that their Co-doping-dependent spin excitations are also similar [47–50], we conclude that magnetism and spin excitations must play a critical role in the pairing mechanisms of iron-based superconductors [4].

ACKNOWLEDGMENTS

The single-crystal growth efforts and neutron scattering work at Rice are supported by the United States DOE, BES, through Contract No. DE-SC0012311 (P.D.). Part of the materials work at Rice University is supported by the Robert A. Welch Foundation through Grant No. C-1839 (P.D.). The neutron scattering work at ORNLs HFIR is sponsored by the Scientific User Facilities Division, Office of Basic Energy Sciences, US Department of Energy. Transport measurements are supported by the National Basic Research Program of China (973 Program, Grant No. 2012CB821401), the National Natural Science Foundation of China (Grant No. 11374011), and the Fundamental Research Funds for the Central Universities (Grant No. 2014KJJCB27).

[1] P. A. Lee, N. Nagaosa, and X.-G. Wen, Rev. Mod. Phys. **78**, 17 (2006).
[2] Y. Kamihara, T. Watanabe, M. Hirano, and H. Hosono, J. Am. Chem. Soc. **130**, 3296 (2008).
[3] C. de la Cruz, Q. Huang, J. W. Lynn, J. Li, W. Ratcliff, II, J. L. Zarestky, H. A. Mook, G. F. Chen, J. L. Luo, N. L. Wang, and P. C. Dai, Nature (London) **453**, 899 (2008).
[4] D. J. Scalapino, Rev. Mod. Phys. **84**, 1383 (2012).
[5] P. C. Dai, Rev. Mod. Phys. **87**, 855 (2015).
[6] J. M. Tranquada, G. Xu, and I. A. Zaliznyak, J. Magn. Magn. Mater. **350**, 148 (2014).
[7] C. Lester, J.-H. Chu, J. G. Analytis, S. C. Capelli, A. S. Erickson, C. L. Condron, M. F. Toney, I. R. Fisher, and S. M. Hayden, Phys. Rev. B **79**, 144523 (2009).

[8] D. K. Pratt, W. Tian, A. Kreyssig, J. L. Zarestky, S. Nandi, N. Ni, S. L. Bud'ko, P. C. Canfield, A. I. Goldman, and R. J. McQueeney, Phys. Rev. Lett. **103**, 087001 (2009).

[9] A. D. Christianson, M. D. Lumsden, S. E. Nagler, G. J. MacDougall, M. A. McGuire, A. S. Sefat, R. Jin, B. C. Sales, and D. Mandrus, Phys. Rev. Lett. **103**, 087002 (2009).

[10] S. Nandi, M. G. Kim, A. Kreyssig, R. M. Fernandes, D. K. Pratt, A. Thaler, N. Ni, S. L. Budko, P. C. Canfield, J. Schmalian, R. J. McQueeney, and A. I. Goldman, Phys. Rev. Lett. **104**, 057006 (2010).

[11] D. K. Pratt, M. G. Kim, A. Kreyssig, Y. B. Lee, G. S. Tucker, A. Thaler, W. Tian, J. L. Zarestky, S. L. Bud'ko, P. C. Canfield, B. N. Harmon, A. I. Goldman, and R. J. McQueeney, Phys. Rev. Lett. **106**, 257001 (2011).

[12] H. Luo, R. Zhang, M. Laver, Z. Yamani, M. Wang, X. Lu, M. Wang, Y. Chen, S. Li, S. Chang, J. W. Lynn, and P. Dai, Phys. Rev. Lett. **108**, 247002 (2012).

[13] X. Lu, H. Gretarsson, R. Zhang, X. Liu, H. Luo, W. Tian, M. Laver, Z. Yamani, Y.-J. Kim, A. H. Nevidomskyy, Q. Si, and P. Dai, Phys. Rev. Lett. **110**, 257001 (2013).

[14] T. Shibauchi, A. Carrington, and Y. Matsuda, Annu. Rev. Condens. Matter Phys. **5**, 113 (2014).

[15] J. G. Analytis, H.-H. Kuo, R. D. McDonald, M. Wartenbe, P. M. C. Rourke, N. E. Hussey, and I. R. Fisher, Nat. Phys. **10**, 194 (2014).

[16] Y. Nakai, T. Iye, S. Kitagawa, K. Ishida, H. Ikeda, S. Kasahara, H. Shishido, T. Shibauchi, Y. Matsuda, and T. Terashima, Phys. Rev. Lett. **105**, 107003 (2010).

[17] J. M. Allred, K. M. Taddei, D. E. Bugaris, S. Avci, D. Y. Chung, H. Claus, C. de la Cruz, M. G. Kanatzidis, S. Rosenkranz, R. Osborn, and O. Chmaissem, Phys. Rev. B **90**, 104513 (2014).

[18] D. Hu, X. Lu, W. Zhang, H. Luo, S. Li, P. Wang, G. Chen, F. Han, S. R. Banjara, A. Sapkota, A. Kreyssig, A. I. Goldman, Z. Yamani, C. Niedermayer, M. Skoulatos, R. Georgii, T. Keller, P. Wang, W. Yu, and P. Dai, Phys. Rev. Lett. **114**, 157002 (2015).

[19] N. Ni, A. Thaler, J. Q. Yan, A. Kracher, E. Colombier, S. L. Bud'ko, P. C. Canfield, and S. T. Hannahs, Phys. Rev. B **82**, 024519 (2010).

[20] S. Kasahara, T. Shibauchi, K. Hashimoto, K. Ikada, S. Tonegawa, R. Okazaki, H. Shishido, H. Ikeda, H. Takeya, K. Hirata, T. Terashima, and Y. Matsuda, Phys. Rev. B **81**, 184519 (2010).

[21] S. Avci, O. Chmaissem, J. M. Allred, S. Rosenkranz, I. Eremin, A. V. Chubukov, D. E. Bugaris, D. Y. Chung, M. G. Kanatzidis, J.-P Castellan, J. A. Schlueter, H. Claus, D. D. Khalyavin, P. Manuel, A. Daoud-Aladine, and R. Osborn, Nat. Commun. **5**, 3845 (2014).

[22] F. Waßer, A. Schneidewind, Y. Sidis, S. Wurmehl, S. Aswartham, B. Buchner, and M. Braden, Phys. Rev. B **91**, 060505(R) (2015).

[23] J. M. Allred, K. M. Taddei, D. E. Bugaris, M. J. Krogstad, S. H. Lapidus, D. Y. Chung, H. Claus, M. G. Kanatzidis, D. E. Brown, J. Kang, R. M. Fernandes, I. Eremin, S. Rosenkranz, O. Chmaissem, and R. Osborn, Nat. Phys. **12**, 493 (2016).

[24] Q. Huang, Y. Qiu, W. Bao, M. A. Green, J. W. Lynn, Y. C. Gasparovic, T. Wu, G. Wu, and X. H. Chen, Phys. Rev. Lett. **101**, 257003 (2008).

[25] D. R. Parker, M. J. Pitcher, P. J. Baker, I. Franke, T. Lancaster, S. J. Blundell, and S. J. Clarke, Chem. Commun. (Cambridge) 2189, (2009).

[26] D. R. Parker, M. J. P. Smith, T. Lancaster, A. J. Steele, I. Franke, P. J. Baker, F. L. Pratt, M. J. Pitcher, S. J. Blundell, and S. J. Clarke, Phys. Rev. Lett. **104**, 057007 (2010).

[27] J. D. Wright, T. Lancaster, I. Franke, A. J. Steele, J. S. Möller, M. J. Pitcher, A. J. Corkett, D. R. Parker, D. G. Free, F. L. Pratt, P. J. Baker, S. J. Clarke, and S. J. Blundell, Phys. Rev. B **85**, 054503 (2012).

[28] A. F. Wang, X. G. Luo, Y. J. Yan, J. J. Ying, Z. J. Xiang, G. J. Ye, P. Cheng, Z. Y. Li, W. J. Hu, and X. H. Chen, Phys. Rev. B **85**, 224521 (2012).

[29] A. F. Wang, J. J. Ying, X. G. Luo, Y. J. Yan, D. Y. Liu, Z. J. Xiang, P. Cheng, G. J. Ye, L. J. Zou, Z. Sun, and X. H. Chen, New J. Phys. **15**, 043048 (2013).

[30] G. Tan, P. Zheng, X. Wang, Y. Chen, X. Zhang, J. Luo, T. Netherton, Y. Song, P. Dai, C. Zhang, and S. Li, Phys. Rev. B **87**, 144512 (2013).

[31] S. Li, C. de la Cruz, Q. Huang, G. F. Chen, T.-L. Xia, J. L. Luo, N. L. Wang, and P. C. Dai, Phys. Rev. B **80**, 020504(R) (2009).

[32] C. Zhang, H.-F. Li, Y. Song, Y. Su, G. Tan, T. Netherton, C. Redding, S. V. Carr, O. Sobolev, A. Schneidewind, E. Faulhaber, L. W. Harriger, S. Li, X. Lu, D.-X. Yao, T. Das, A. V. Balatsky, Th. Brückel, J. W. Lynn, and P. Dai, Phys. Rev. B **88**, 064504 (2013).

[33] R. Zhang, D. L. Gong, X. Y. Lu, S. L. Li, M. Laver, Ch. Niedermayer, S. Danilkin, G. C. Deng, P. C. Dai, and H. Q. Luo, Phys. Rev. B **91**, 094506 (2015).

[34] A. Rosch, Phys. Rev. Lett. **82**, 4280 (1999).

[35] R. A. Cooper, Y. Wang, B. Vignolle, O. J. Lipscombe, S. M. Hayden, Y. Tanabe, T. Adachi, Y. Koike, M. Nohara, H. Takagi, C. Proust, and N. E. Hussey, Science **323**, 603 (2009).

[36] H. v. Löhneysen, A. Rosch, M. Vojta, and P. Wölfle, Rev. Mod. Phys. **79**, 1015 (2007).

[37] N. Spyrison, M. A. Tanatar, Kyuil Cho, Y. Song, P. Dai, C. Zhang, and R. Prozorov, Phys. Rev. B **86**, 144528 (2012).

[38] A. P. Dioguardi, J. Crocker, A. C. Shockley, C. H. Lin, K. R. Shirer, D. M. Nisson, M. M. Lawson, N. apRoberts-Warren, P. C. Canfield, S. L. Bud'ko, S. Ran, and N. J. Curro, Phys. Rev. Lett. **111**, 207201 (2013).

[39] X. Y. Lu, D. W. Tam, C. Zhang, H. Luo, M. Wang, R. Zhang, L. W. Harriger, T. Keller, B. Keimer, L.-P. Regnault, T. A. Maier, and P. C. Dai, Phys. Rev. B **90**, 024509 (2014).

[40] A. P. Dioguardi, M. M. Lawson, B. T. Bush, J. Crocker, K. R. Shirer, D. M. Nisson, T. Kissikov, S. Ran, S. L. Bud'ko, P. C. Canfield, S. Yuan, P. L. Kuhns, A. P. Reyes, H.-J. Grafe, and N. J. Curro, Phys. Rev. B **92**, 165116 (2015).

[41] A. Kreyssig, M. G. Kim, S. Nandi, D. K. Pratt, W. Tian, J. L. Zarestky, N. Ni, A. Thaler, S. L. Bud'ko, P. C. Canfield, R. J. McQueeney, and A. I. Goldman, Phys. Rev. B **81**, 134512 (2010).

[42] X. Y. Lu, J. T. Park, R. Zhang, H. Q. Luo, A. H. Nevidomskyy, Q. Si, and P. C. Dai, Science **345**, 657 (2014).

[43] P. Richard, T. Sato, K. Nakayama, T. Takahashi, and H. Ding, Rep. Prog. Phys. **74**, 124512 (2011).

[44] Z.-H. Liu, P. Richard, K. Nakayama, G.-F. Chen, S. Dong, J.-B. He, D.-M. Wang, T.-L. Xia, K. Umezawa, T. Kawahara, S. Souma, T. Sato, T. Takahashi, T. Qian, Y. Huang, N. Xu, Y. Shi, H. Ding, and S.-C. Wang, Phys. Rev. B **84**, 064519 (2011).

[45] S. T. Cui, S. Y. Zhu, A. F. Wang, S. Kong, S. L. Ju, X. G. Luo, X. H. Chen, G. B. Zhang, and Z. Sun, Phys. Rev. B **86**, 155143 (2012).

[46] Q. Q. Ge, Z. R. Ye, M. Xu, Y. Zhang, J. Jiang, B. P. Xie, Y. Song, C. L. Zhang, P. C. Dai, and D. L. Feng, Phys. Rev. X **3**, 011020 (2013).

[47] H. Q. Luo, Z. Yamani, Y. Chen, X. Lu, M. Wang, S. Li, T. A. Maier, S. Danilkin, D. T. Adroja, and P. C. Dai, Phys. Rev. B **86**, 024508 (2012).

[48] H. Q. Luo, X. Y. Lu, R. Zhang, M. Wang, E. A. Goremychkin, D. T. Adroja, S. Danilkin, G. Deng, Z. Yamani, and P. C. Dai, Phys. Rev. B **88**, 144516 (2013).

[49] C. L. Zhang, W. C. Lv, G. T. Tan, Y. Song, S. V. Carr, S. X. Chi, M. Matsuda, A. D. Christianson, J. A. Fernandez-Baca, L. W. Harriger, and P. C. Dai, Phys. Rev. B **93**, 174522 (2016).

[50] S. V. Carr, C. L. Zhang, Y. Song, G. T. Tan, Y. Li, D. L. Abernathy, M. B. Stone, G. E. Granroth, T. G. Perring, and P. C. Dai, Phys. Rev. B **93**, 214506 (2016).